International Journal of Pure and Applied Physics
ISSN 0973-1776 Volume 5, Number 3 (2009), pp. 215–229

http://www.ripublication.com/ijpap.htm

Density of States of Rare-earth Permanent Magnet $Nd_2Fe_{14}B$ Using Spin-orbit Coupling

Abeer E Aly[1,*]

[1]*Physics, Faculty of Science at Damieta, Mansoura University, New Damieta, Egypt*
**Corresponding author: abeerresmat782000@yahoo.com*

Abstract

The electronic structures of $Nd_2Fe_{14}B$ are calculated using first-principles full-potential linearized augmented plane wave (FPLAPW) method. We study the effect of considering the spin–orbit coupling and Coulomb correlations in the $Nd_2Fe_{14}B$ on the magnetic properties and the electronic structure. Results are presented for total density of states (DOS) as well as the site-projected partial density of states (PDOS), the spin magnetic moment of Fe at each of the six in-equivalent transition-metal sites and charge-spin density maps. The total spin-magnetic moments and the average Fe moment are in a good agreement with the values deduced from the neutron scattering experiment and the LDA + U + SO scheme is used. The spin-polarized calculations, excluding the Hubbard and SO interaction, resulted in the total spin magnetic moment is 46.6 μ_B compared to the experimental values 34.63 μ_B to the value of 39.6 μ_B we obtained using LDA+U scheme without Spin-Orbit coupling(SO). But using LDA+U +SO the total spin magnetic moment is 37.6. Including the spin-orbit coupling are necessary for getting a better agreement with experimental data. The charge density map and the spin density maps are calculated on the basal and (110) plane of the tetragonal cell.

Introduction

The discovered $Nd_2Fe_{14}B$ has great interest for significant technological applications [1].It has considered a good permanent magnet because it have a large saturation magnetization , larger energy products ,coercivity and high curie temperature[2] . These compounds have complex tetragonal structures with 68 atoms per unit cell .And the fundamental role in the determining the magnetic properties are a good understanding of the electronic structure of these materials. So it is necessary to understand the origin of magnetism in $Nd_2Fe_{14}B$. $Nd_2Fe_{14}B$ is the most important alloy in the series in terms of practical applications and is the one most intensively

studied [3]. Furthermore, study of the location of f-electron levels in rare earth intermetallics and their interaction with the transition-metal conduction band is still in a rather primitive state and should be a subject of considerable interest. Some empirical and non-self consistent calculations have been reported on the electronic structure of $Nd_2Fe_{14}B$ [4-10]. One of these calculations for Inoue and Shimizu [4], Itoh et al.[5], and Szpunar, Wallace, and Szpunar [6] used a semi-empirical tight binding and the recursion method and found that Fe atoms at the j_2 site have the largest magnetic moments and were included spin-polarized only. No studies up to our knowledge were devoted to studying the effect of the spin-orbit coupling on the electronic structure and the density of states (DOS) of $Nd_2Fe_{14}B$ using self-consistent Full Potential Linearized Augmented Plane Wave (FPLAPW) method based on Density Functional Theory (DFT) [11]. This method is based on local-density approximation. The potential and the electron density are separated into two regions, i.e. inside the non-overlapping atomic spheres (region I) and the interstitial regions (region II). The wave function solutions of the Kohn-Sham equation are expanded in augmented wave functions. In region I, they are expanded in radial functions times spherical harmonics. In the interstitial region II, plane wave's expansion is used. Each plane wave is augmented by an atomic-like function inside the atomic sphere and matched at the atomic boundary. However, there is no shape restriction on the density and potential.

The potential in LAPW method:

The LAPW method expands the potential in the following form

$$V(r)=\begin{cases}\sum_{Lm} V_{Lm}(r)Y_{Lm}(\hat{r}) & \text{Inside sphere}\\ \sum_{K} V_K e^{iKr} & \text{Outside sphere}\end{cases} \qquad 1$$

and the charge densities analogously. Thus no shape approximations are made, a procedure frequently called the ``full-potential`` method. The ``muffin-tin`` approximation used in early band calculations corresponds to retaining only the L=0 and M=0 component in the first expression of equation (1) (inside sphere) and only the K=0 component in the second (outside sphere). This procedure corresponds to taking the spherical average inside the spheres and the volume average in the interstitial region. In this paper, we present the calculations of density of states, spin magnetic moment and spin-charge density maps on $Nd_2Fe_{14}B$ using FPLAPW method and different schemes.

Method of Calculations

$Nd_2Fe_{14}B$ crystal are tetragonal unit cell with a space group $P4_2/mnm$, structure No. 136 has two different R sites Nd(f) and Nd(g), six distinct Fe sites (labeled c, e, j_1, j_2, k_1, and k_2, respectively) and one B site for a total of 68 atoms per unit cell [ref 12] . In one unit cell , there are two kinds of 8Nd atoms, labeled as 4Nd(f) and 4Nd(g), respectively, six kinds of 56 Fe atoms, labeled as Fe(c), Fe(e), Fe(j_1), Fe(j_2), Fe(k_1), Fe(k_2), respectively, and only one kind of 4B atoms, labeled as B(g). Near-neighbor Fe-Fe distances in the structure are between 2.4 and 2.8 A and the B atoms are known

to play an important role in bonding[12]. Since they occupy the centers of the trigonal prisms which are formed by 6 neighbor Fe atoms .One Fe(e) and two Fe(k_1) atoms above and one Fe(e) and two Fe(k_1) atoms below and three Nd atoms[2Nd(f) and 1Nd(g)] are bonded to each B atom through the three vertical prism faces. It is clear from the prisms are strong structural units linking the Fe planes above and below those containing Nd and B. The atomic–structure information was taken from ref [12]. We have used the lattice constants and the fourteen atomic position parameters for $Nd_2Fe_{14}B$ at 77K [13].The experimental values used in our calculation are a = 8.802, c= 12.179 A_0[7,8]. The Local Density Approximation (LDA+U) of Perdew and Wang [14] and the Generalized Gradient Approximation (GGA) of Perdew, Burke and Ernzerhof [15] were used for correlations and exchange potentials as implemented in the Wien2k code [16]. Self-consistent calculations were performed with 30 k-points in the irreducible Brillouin zone. We used the muffin tin (MT) sphere radii $R_{MT}^{Nd} = 2.5$ a.u, $R_{MT}^{Fe} = 2.09$ a.u, $R_{MT}^{B} = 1.85$ a.u and the cut off energy parameters RKmax and Gmax of 7 and 14 respectively. There are two very important crystallographic planes in tetragonal cell of $Nd_2Fe_{14}B$ [ref 7,8]: the basal plane (z=0) which contains the two R, B, and Fe(c) sites, and the (110) plane which is parallel to the c axis and contains Fe(e) and Fe(j_1) sites in addition to B and R sites [12]. The charge and spin density of these two planes also are plotted as contour maps for the $Nd_2Fe_{14}B$ calculated in this paper. The total charge density and the spin density are obtained by taking the sum or the difference of the spin-up and spin-dn charge density, respectively. The near-neighbor distances were used to estimate the Wigner-Seitz radii. 4f states in rare earths are highly localized and are very difficult to include the band-structure calculation. Fortunately, their photoemission spectra are reasonable well understood with transition-state analysis [17,18] and renormalized-atom approach [19]. Because of this and the fact that the non-4f parts of the experimental electronic structure are similar 4f states in $Nd_2Fe_{14}B$ were included in the valence and core states. Both core and valence states are the frozen self-consistent atomic states. There are nine valence states per site consisting of s, p and d orbitals. With 68 atoms per unit cell, this leads to 612×612 overlap and Hamiltonian matrices. The self-consistent spin-polarized potential parameters are based on the zero-wave-vector (K~0) electronic structure results. Because of the extremely large size of the unit cell so in our work, the Nd f electrons are considered as valence electrons and are treated self-consistently. Furthermore, we have used a small FPLAPW basis set for Nd atoms and small k-points for the Brillouin-zone integration.

Results and Discussion

To describe the electronic and magnetic properties of $Nd_2Fe_{14}B$, we have used the self-consistent Full Potential Linearized Augmented Plane Wave (FPLAPW) .Both core and valence states are calculated self-consistently, the core states are treated fully relativistically for the spherical part of the potential, whereas the full potential is used for the valence states. In our work, the Nd *f* electrons are considered as valence electrons. First, here we performed spin-polarized calculation on $Nd_2Fe_{14}B$ after that

adding LDA+U with and without spin-orbit coupling. LDA is due to the localized nature of f-electrons as well as to the subtle interplay between the spin polarization and the spin-orbit interaction. The orbital magnetic moment is caused by the spin-orbit coupling and also by the correlation effects, the latter effects being more important. LDA+U method [11] will be useful because the LDA+U, removes the deficiency of LDA by incorporating the Hubbard-like interaction term for 4f electrons.

A. Spin-Polarized only

We performed spin-polarized calculations on $Nd_2Fe_{14}B$, excluding the Hubbard and SO interaction. We calculated the spin magnetic moment $Ms(\mu_B)$ as shown in table I . The magnetic moments $Ms(\mu_B)$ for the Fe sites are 2.39,2.37,2.36,2.43,2.40,2.38 μ_B for the k_1, k_2, j_1, j_2, e and c sites respectively . These numbers are in a good agreement with the experimental values of 2.60, 2.60, 2.30, 2.85, 2.10, 2.75 μ_B respectively [20,21].The Fe-site moments are in agreement with two reported results of neutron-scattering experiments, one on single crystals [20] and another on powder samples [21] . Szpunar et al [6], Inoue et al and Shimizu et al [4] and Itoh et al [5] used a semi-empirical tight binding and the recursion method and found that Fe atoms at j_2 site have the largest magnetic moments. Using the spin-polarized only we found the largest Fe magnetic moment at the j_2 site, but the smallest Fe magnetic moment at the j_1 site. Figs. (1, 2) show the majority and minority density of states (DOS) and the orbital-decomposed (PDOS). The total DOS spin-up for $Nd_2Fe_{14}B$ in Fig.(1a) is dominated by the Fe 3d-states as shown in Fig.(1c) . The peaks in Fig.(1c) are located from ~ 0 to ~ -5 eV .The highly localized Nd (4f ,4g) peaks are found to be located clustered around the E_f as shown in Fig.(1b) and the low two peaks located at ~ -9 eV due to B states as shown in Fig.(1d) .While the total DOS spin-dn for $Nd_2Fe_{14}B$ in Fig.(2a) is dominated by the Fe 3d-states as shown in Fig.(2c). The peaks in Fig.(2c) are located from ~ 3 to ~ -3 eV .The highly localized Nd (4f ,4g) peaks are found to be above the E_f as shown in Fig.(2b) and the low two peaks located from ~ -7 and ~ -8 eV due to B states as shown in Fig.(2d). From Fig.(1c,2c) it also becomes clear why the j_2 site has the largest magnetic moment. At the j_2 site the major peak of the majority-spin is just below the E_f, while most of the minority spin is above the E_f resulting in a large spin magnetic moment. The site-decomposed spin-magnetic moments at different Fe site for $Nd_2Fe_{14}B$ are summarized in table I. The significantly different PDOS curves indicate strong local environment differences at different Fe site. The average Fe moment is 2.38 μ_B compared to the experimental values ~ 2.57μ_B [21,22]. We calculated the total magnetic moment of ~ 46.62μ_B using this scheme which is larger than the experimental value of ~35.0 μ_B/f.u or 37.1 μ_B /f.u [21,22] and this demonstrates that the spin-polarized scheme is not suitable for handling f-systems. And the density of states (DOS) in Fig.(1c) show that the 3d-state of Fe atoms has the largest peak at the c site instead of the j_2 site. So this shows the importance of including LDA+U plus SO as we will show in the next part.

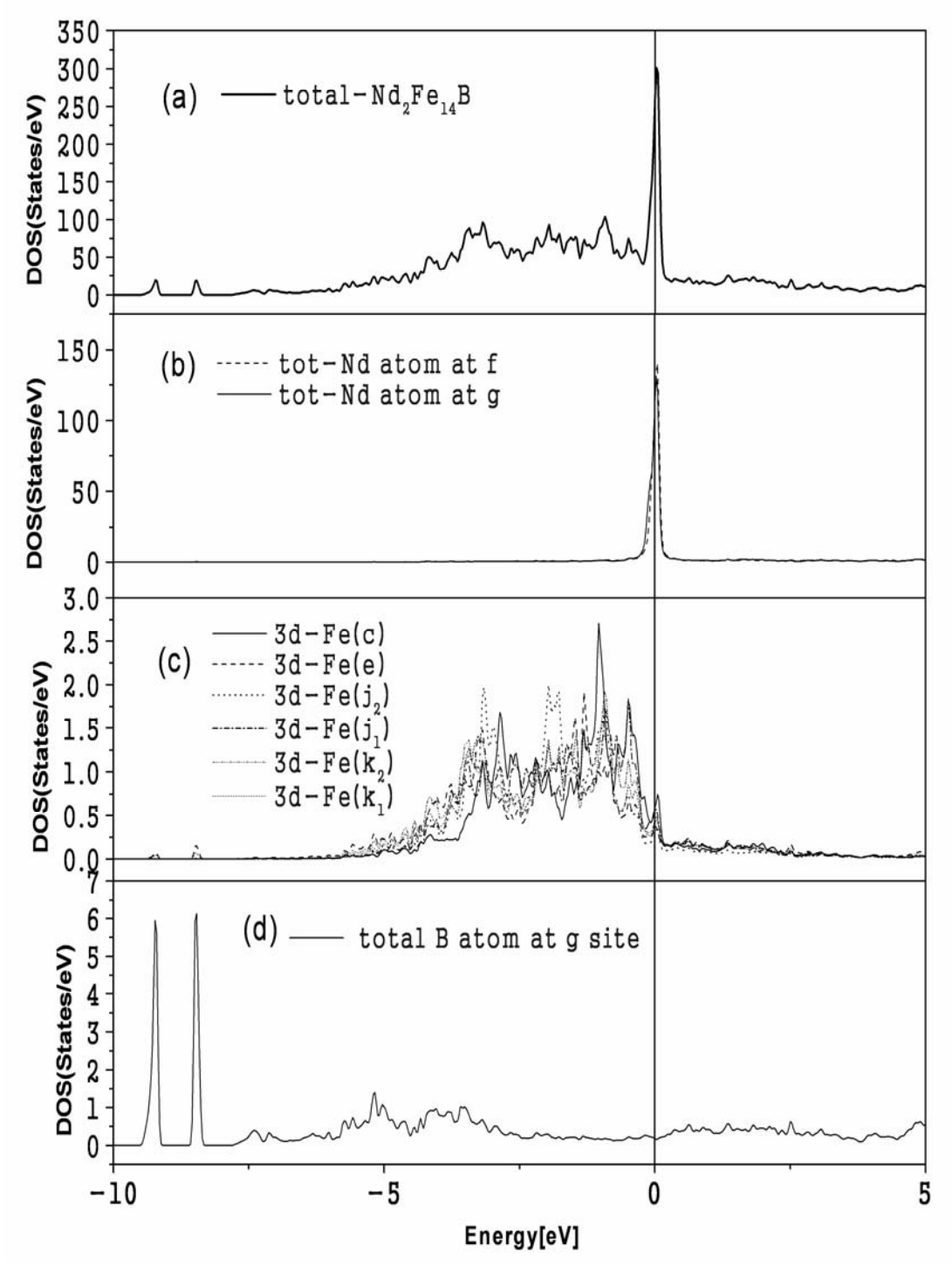

Figure 1: Total and PDOS spin-up density of states (DOS) for Nd2Fe14B, (a)Total density of states (DOS)(spin-up) of $Nd_2Fe_{14}B$; (b) density of states (DOS) of 2Nd f state at f and g sites; (c) density of states(DOS) of six types of Fe atoms ;(d) Total density of states (DOS) of B atom .Using spin-polarized.

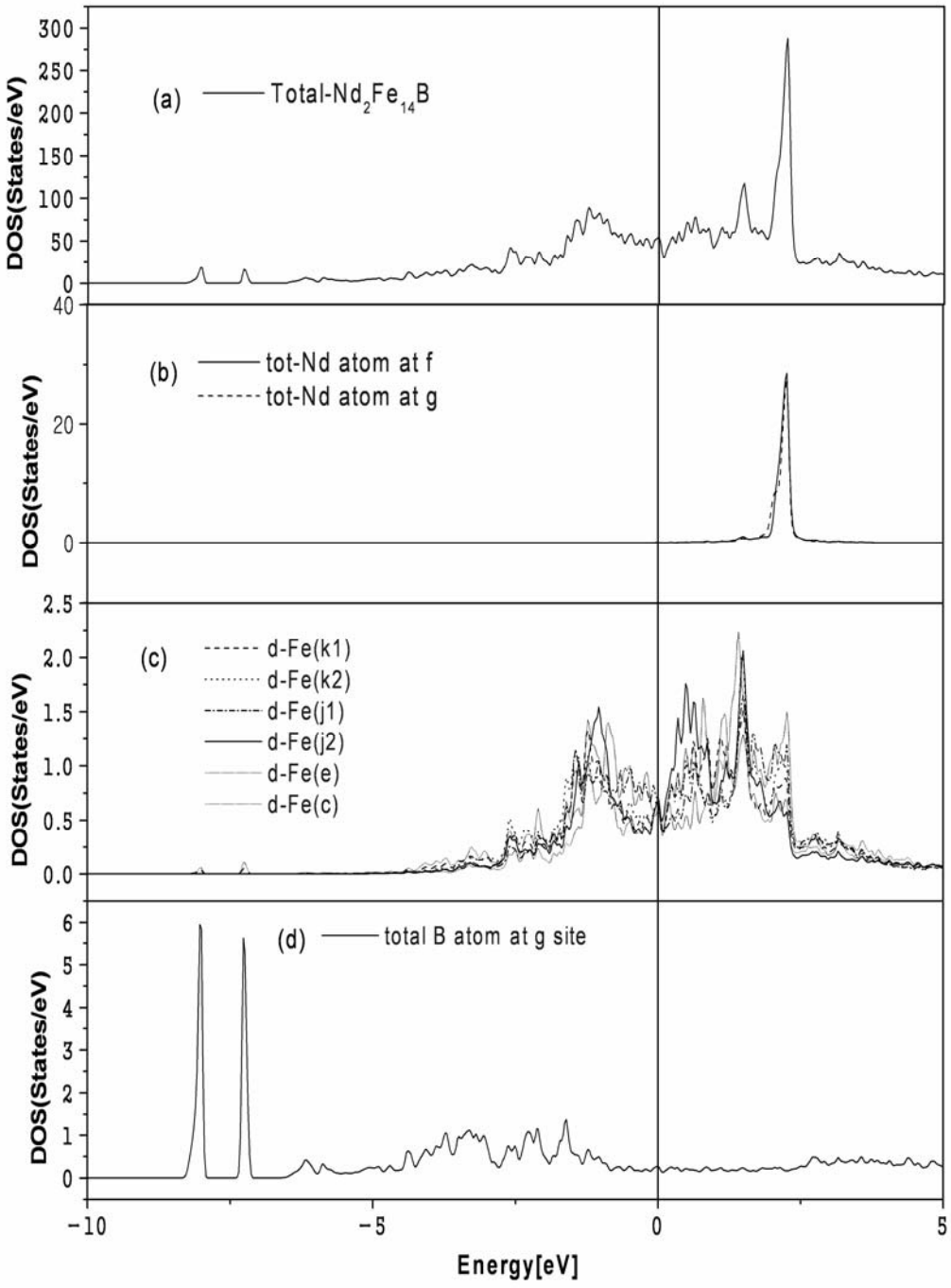

Figure 2: Total and PDOS spin-dn density of states (DOS) for Nd2Fe14B, (a)Total density of states (DOS)(spin-up) of $Nd_2Fe_{14}B$; (b) density of states (DOS) of 2Nd f state at f and g sites; (c) density of states(DOS) of six types of Fe atoms ;(d) Total density of states (DOS) of B atom .Using spin-polarized.

Table I: spin magnetic moment $Ms(\mu_B)$, at each atomic sites in $Nd_2Fe_{14}B$ using spin-polarized.

	$Fe(k_1)$	$Fe(k_2)$	$Fe(j_1)$	$Fe(j_2)$	Fe(e)	Fe(c)
$M_s(\mu_B)$	2.39	2.37	2.36	2.43	2.40	2.38
$M_s(\mu_B)$ Exp(Ref 20,21)	2.60	2.60	2.30	2.85	2.10	2.75

B. LDA+U without spin-orbit coupling

Using LDA+U without spin-orbit coupling we calculated the spin magnetic moment $Ms(\mu_B)$ as shown in table II. The magnetic moments $Ms(\mu_B)$ for the Fe sites are 2.25,2.28,2.24,2.58,2.18,2.3 μ_B for the k_1, k_2, j_1, j_2, e and c sites respectively. These numbers are to be compared with experimental values of 2.60, 2.60, 2.30, 2.85, 2.10, 2.75 μ_B respectively [20,21]. The agreement between the theoretical calculation and experimental values is observed. The largest Fe moment is found at the j_2 site as before, but the smallest Fe moment is at the e site. Fig. (3b) show that the localized Nd(4f) (spin-up) peak is found to be shifted above the E_f and splitting above and below E_f while the Nd (4f) spin-dn the peaks is found to be located above the E_f and splitting as shown in Fig.(4b) using LDA+U+SO. We also note that Nd (4f) peak at g site is larger than the Nd (4g) peak at f site as shown in Fig.(3b).Figs. (3,4) show the majority and minority total density of states (DOS) and the orbital-decomposed (PDOS) . The total DOS spin-up for $Nd_2Fe_{14}B$ in Fig.(3a) is dominated by the Fe 3d-states as shown in Fig.(3c). The peaks in Fig.(3c) are located from ~ -1 to ~ -5 eV. The highly localized Nd (4f ,4g) peaks are found to be located above and below the E_f as shown in Fig.(3b) and the low two peaks located at ~ -9 eV due to B states as shown in Fig.(3d) .While the total DOS spin-dn for $Nd_2Fe_{14}B$ in Fig.(4a) is dominated by the Fe 3d-states as shown in Fig.(4c). The peaks in Fig.(4c) are located from ~ 3 to ~ -3 eV. The highly localized Nd (4f ,4g) peaks are found to be above the E_f as shown in Fig.(4b) and the low two peaks located from ~ -7 and ~ -8 eV due to B states as shown in Fig.(4d).The site-decomposed spin-magnetic moments at each atomic sites for $Nd_2Fe_{14}B$ are summarized in table II. The Fe-site moments are in a good agreement with two reported results of neutron scattering experiments. We calculated the total magnetic moment of ~ $39.62\mu_B$ using this scheme (LDA+U+SO) which is near agreement with the experimental value of ~35.0 μ_B /f.u or 37.1 μ_B /f.u [21,22]. The average Fe moment is 2.31 μ_B compared to the experimental values ~ $2.53\mu_B$ [21,22] .The density of states (DOS) in Fig.(4c) show that the 3d-state of Fe atoms has the largest peak at the c and j_2 sites .So this show the importance of including LDA+U+SO plus spin-orbit coupling as we will show in the next part.

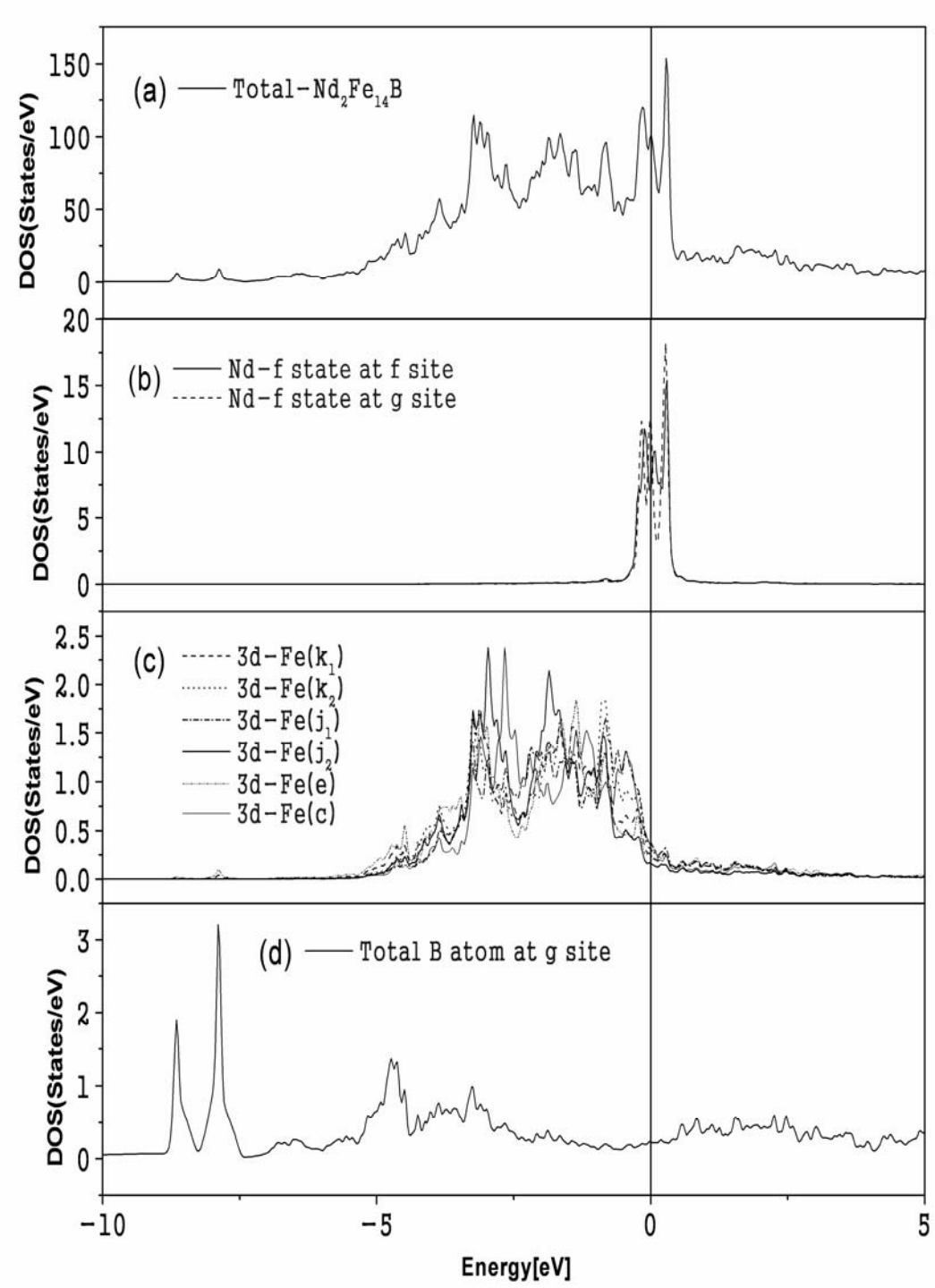

Figure 3: Total and PDOS spin-up density of states (DOS) for Nd2Fe14B, (a)Total density of states (DOS)(spin-up) of $Nd_2Fe_{14}B$; (b) density of states (DOS) of 2Nd f state at f and g sites; (c) density of states(DOS) of six types of Fe atoms ;(d) Total density of states (DOS) of B atom .Using spin-polarized+SO.

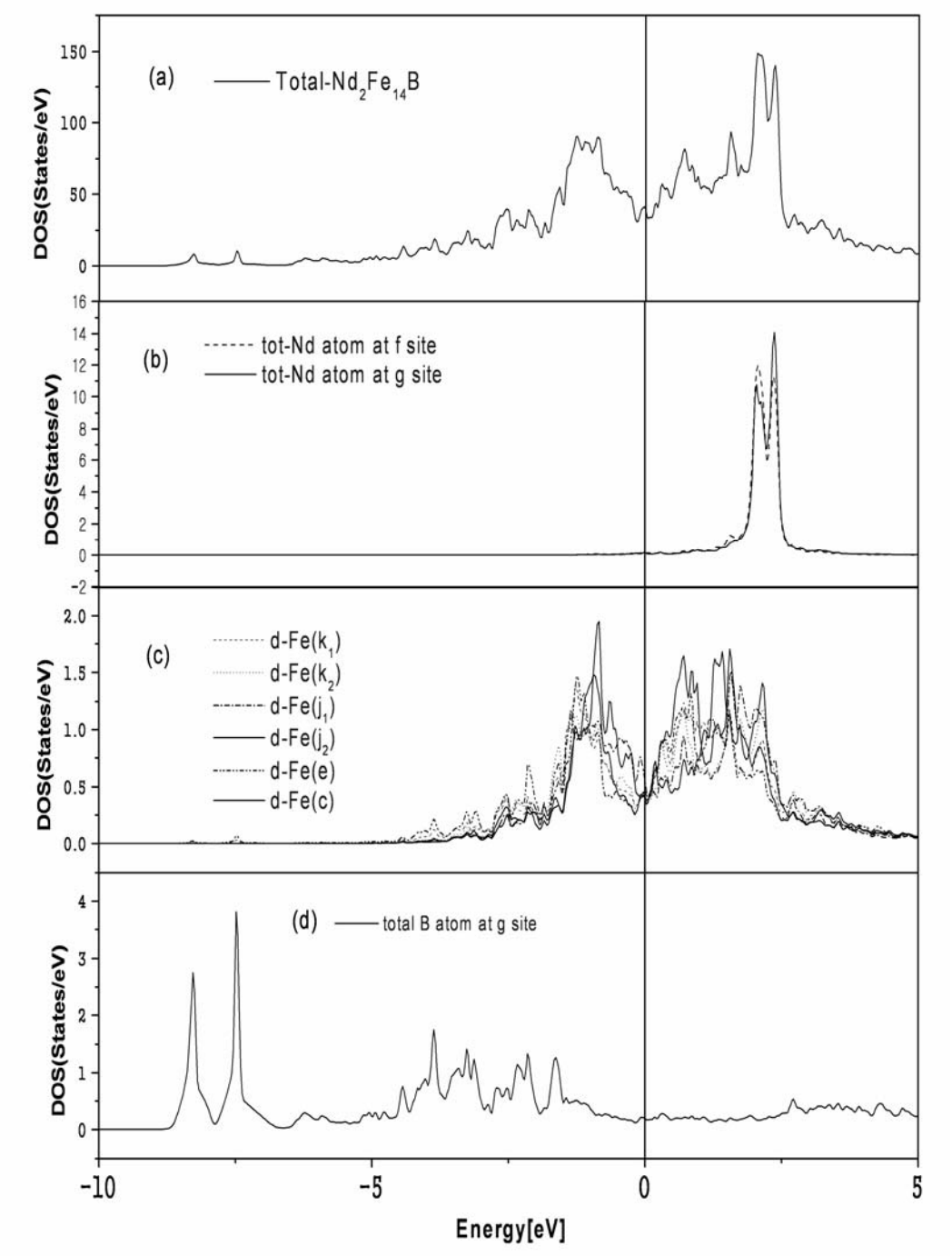

Figure 4: Total and PDOS spin-dn density of states (DOS) for Nd2Fe14B, (a)Total density of states (DOS)(spin-up) of $Nd_2Fe_{14}B$; (b) density of states (DOS) of 2Nd f state at f and g sites; (c) density of states(DOS) of six types of Fe atoms ;(d) Total density of states (DOS) of B atom .Using spin-polarized+SO.

Table II: spin magnetic moment $Ms(\mu_B)$, at each atomic sites in $Nd_2Fe_{14}B$ using spin-LDA+U without SO.

	$Fe(k_1)$	$Fe(k_2)$	$Fe(j_1)$	$Fe(j_2)$	Fe(e)	Fe(c)
$M_s(\mu_B)$	2.25	2.28	2.24	2.58	2.18	2.30
$M_s(\mu_B)$ Exp(Ref 20,21)	2.60	2.60	2.30	2.85	2.10	2.75

C. LDA+U plus Spin-Orbit Coupling(SO)

Using spin-orbit coupling including the Hubbard and exchange parameters (U, J) we calculated the spin magnetic moment $Ms(\mu_B)$ as shown in table III. We obtained $Ms(\mu_B)$**,** values of 2.26,2.38,2.29,2.72,2.15,2.44 μ_B for the k_1, k_2, j_1, j_2, e and c sites respectively . The agreement between the theoretical calculation and experimental values is observed. The largest magnetic moment is found at the j_2 sites of 3d-states of Fe atoms, but the smallest Fe moment is at the e site .Figs. (5,6) show majority and minority total density of states (DOS) and the orbital-decomposed (PDOS). The total DOS spin-up for $Nd_2Fe_{14}B$ in Fig.(5a) is dominated by the Fe 3d-states as shown in Fig.(5c). The peaks in Fig.(5c) are located from ~ -1 to ~ -5 eV. The highly localized Nd (4f ,4g) peaks are found to be located above and below the E_f as shown in Fig.(5b) and the B states is about ~ -9 eV as shown in Fig.(5d) while the total DOS spin-dn for $Nd_2Fe_{14}B$ in Fig.(6a) is dominated by the Fe 3d-states as shown in Fig.(6c).The peaks in Fig.(6c) are located from ~ 3 to ~ -3 eV. The highly localized Nd (4f ,4g) peaks are found to be above the E_f as shown in Fig.(6b) and the low two peaks located from ~ -7 and ~ -8 eV due to B states as shown in Fig.(6d). The site-decomposed spin-magnetic moments at each atomic sites for $Nd_2Fe_{14}B$ are summarized in table III. We calculated the total magnetic moment of ~ $37.61\mu_B$ using spin-orbit coupling which is approximately near the experimental value of ~35.0 μ_B /f.u or 37.1 μ_B /f.u [21,22]. The average Fe moment is 2.38 μ_B compared to the experimental values ~ $2.53\mu_B$ [21,22]. The DOS structure by using spin-orbit coupling are in good agreement with the DOS structure reported by Szpupar et al and Wallace et al, Inoue et al and Shimizu et al and Itoh et al , that they found the largest 3d-state of Fe atoms is through the j_2 site.

Table III: spin magnetic moment $Ms(\mu_B)$ at each atomic sites in $Nd_2Fe_{14}B$ using spin-orbit coupling

	$Fe(k_1)$	$Fe(k_2)$	$Fe(j_1)$	$Fe(j_2)$	Fe(e)	Fe(c)
$M_s(\mu_B)$	2.26	2.38	2.29	2.72	2.15	2.44
$M_s(\mu_B)$ Exp(Ref 20,21)	2.60	2.60	2.30	2.85	2.10	2.75

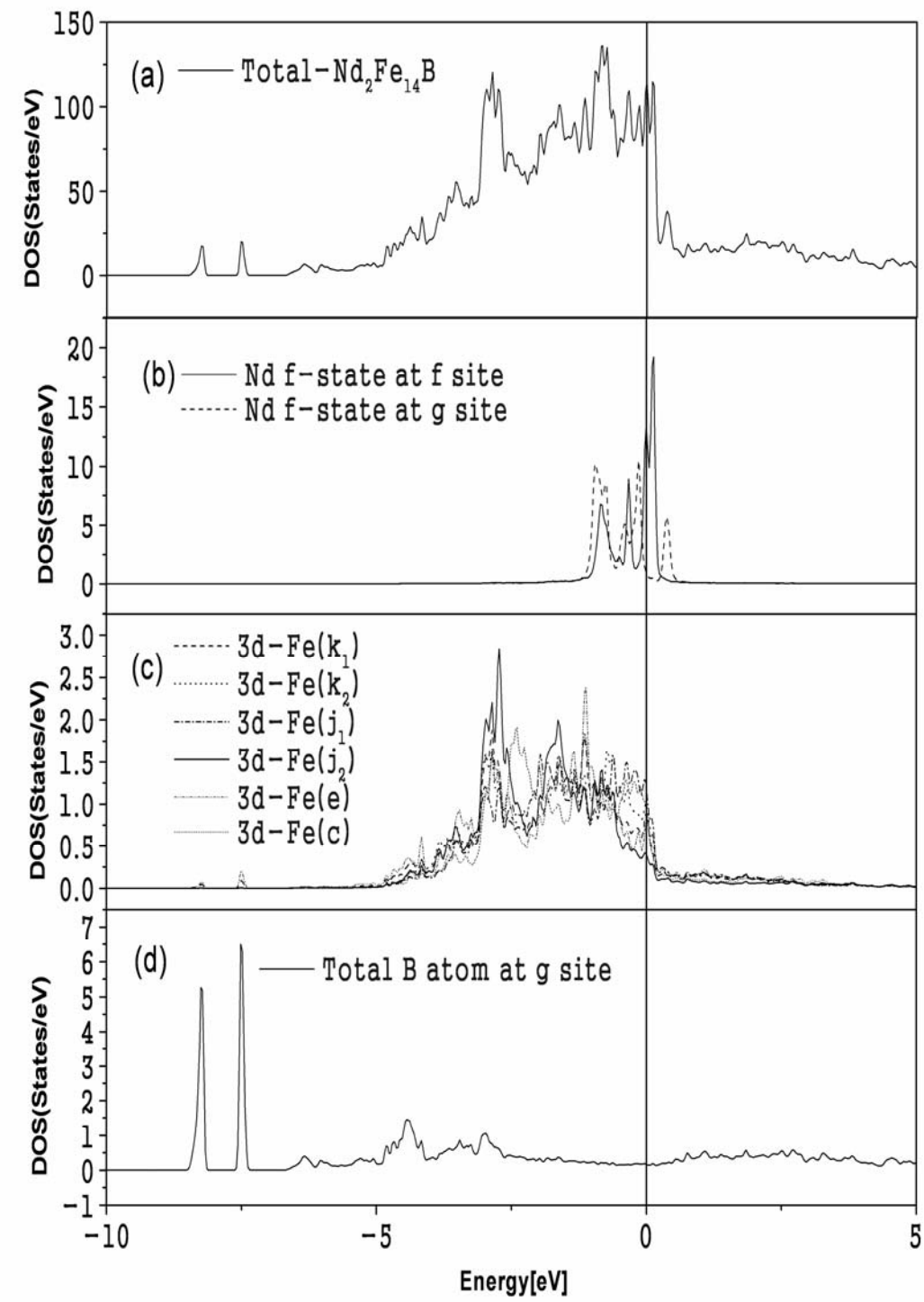

Figure 5: Total and PDOS spin-up density of states (DOS) for Nd2Fe14B, (a)Total density of states (DOS)(spin-up) of $Nd_2Fe_{14}B$; (b) density of states (DOS) of 2Nd f state at f and g sites; (c) density of states(DOS) of six types of Fe atoms ;(d) Total density of states (DOS) of B atom .Using spin-polarized plus SO plus spin-orbit coupling.

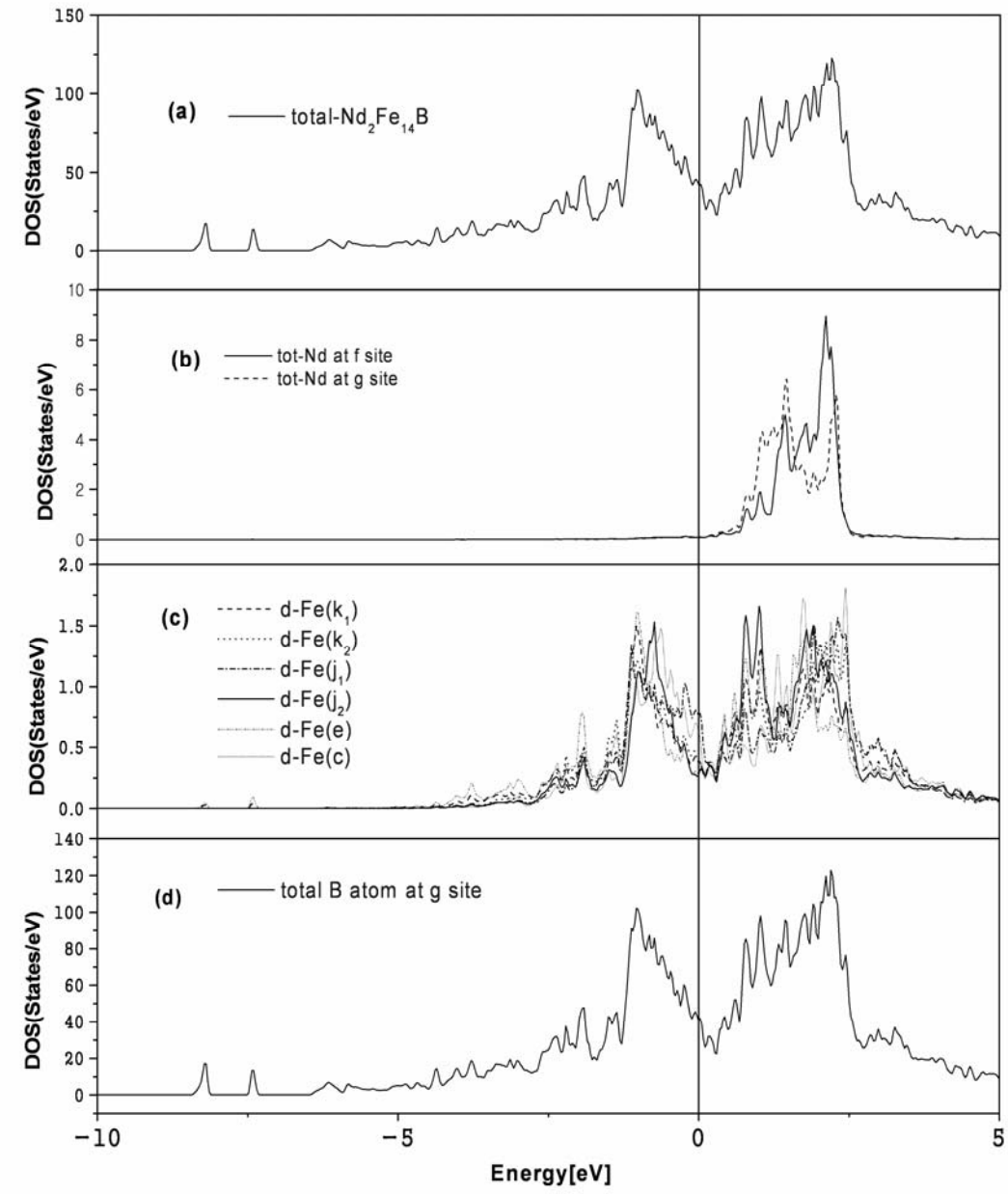

Figure 6: Total and PDOS spin-dn density of states (DOS) for Nd2Fe14B, (a)Total density of states (DOS)(spin-up) of Nd2Fe14B; (b) density of states (DOS) of 2Nd f state at f and g sites; (c) density of states(DOS) of six types of Fe atoms ;(d) Total density of states (DOS) of B atom .Using spin-polarized plus SO plus spin-orbit coupling.

D. Spin and Charge Density Maps

The charge and spin density maps on two plane: basal plane (z=0) which contains the two R,B, and Fe(c) sites, as shown in Fig.(10a from ref 7,8) and the (110) plane which is parallel to the c axis and contains Fe(e) and Fe(j_1) sites in addition to B and R sites as shown in Fig. (11a from ref 7,8). The spin and charge density of $Nd_2Fe_{14}B$ calculated from the difference between spin-up and down densities for spin density and sum between spin-up and down densities for charge density have been plotted in the (001) and (110) planes .We calculated the spin and charge density contours for rare-earth transition metal compounds e.g. $Nd_2Fe_{14}B$ using spin-polarized but without spin-orbit coupling. The contours used in the plots with an interval of 0.1.The crystallographic (001) basal plane in $Nd_2Fe_{14}B$ shown in Fig.(7a).The charge density contours in a portion of the (001) plane containing two Nd(g) , two Nd(f), four Fe(c) and two B(g) as in Fig.(7b) and the spin density contours in a portion of the (001) plane containing two Nd(g) , two Nd(f), four Fe(c) and disappear the two B(g) as In Fig.(7c).The crystallographic (110) plane in $Nd_2Fe_{14}B$ shown in Fig.(8a). The charge density contours in a portion of the (110) plane containing two Nd(g) , two Nd(f), four B(g), six Fe(e), four Fe(j_2) and four Fe(j_1) as in fig(8b) and the spin density contours in a portion of the (110) plane containing two Nd(g) , two Nd(f), six Fe(e), four Fe(j_2) and four Fe(j_1) and disappear the four B(g) as in Fig(8c).

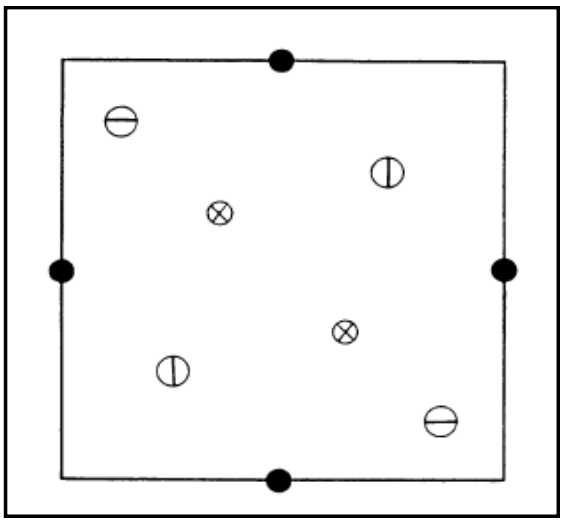

Figure 7 a: Crystallographic (001) basal plane in $Nd_2Fe_{14}B$.

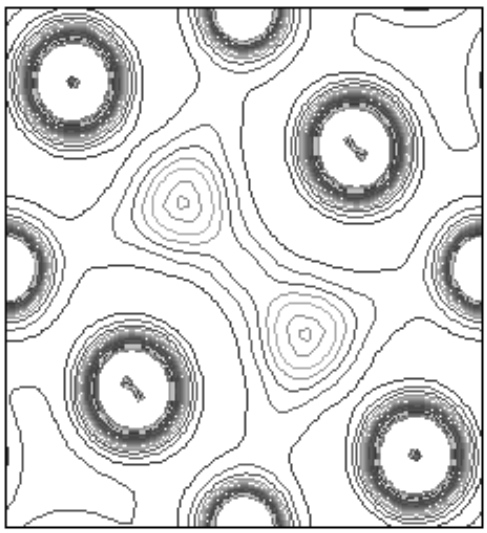

Figure 7 b: Charge density of $Nd_2Fe_{14}B$ on (001) basal plane.

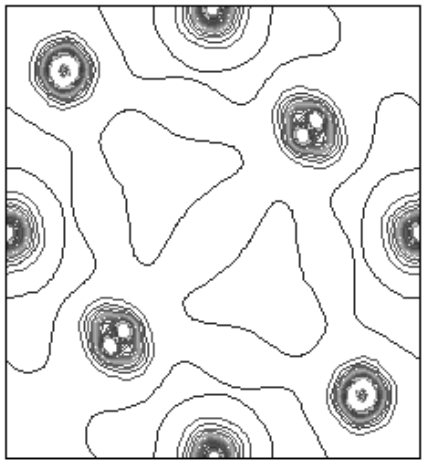

Figure 7c: spin density of $Nd_2Fe_{14}B$ on (001) basal plane.

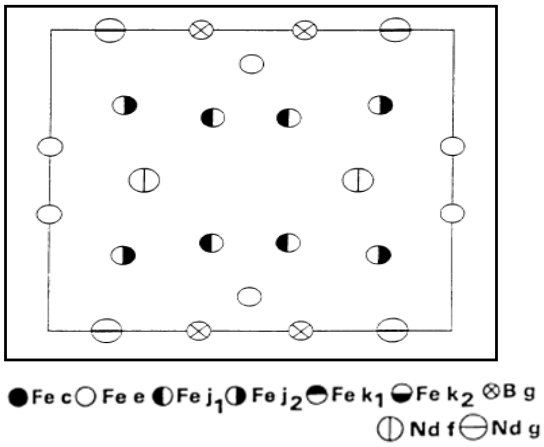

Figure 8 a: Crystallographic (110) plane in $Nd_2Fe_{14}B$.

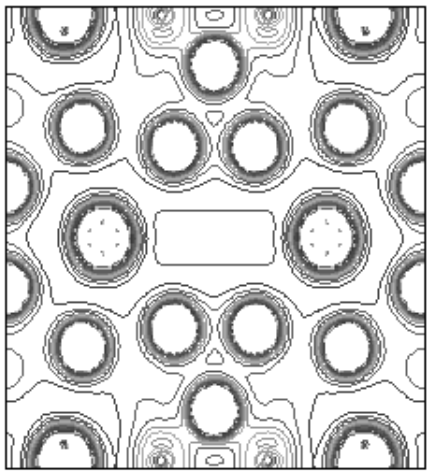

Figure 8b: Charge density of $Nd_2Fe_{14}B$ on (110) plane.

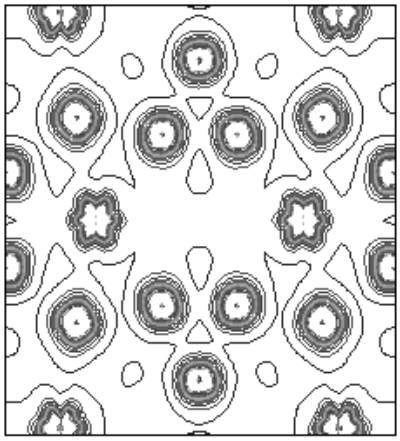

Figure 8c: spin density of $Nd_2Fe_{14}B$ on (110) plane.

Conclusions

We have performed ab initio calculation on the electronic structure of $Nd_2Fe_{14}B$ intermetallic alloys using full potential linearized augmented plane wave (FPLAPW) method based on DFT theory and different interaction schemes available in the Wien2k code. The magnetic moment are best described in the LDA + U + SO scheme as shown by comparison with available calculations and experiments on Nd2Fe14B. The agreement is quite good in that it correctly predict that the largest sites are at j2 site. We also presented the charge and the spin density maps on the basal and (110) plane.

References

[1] J. F. Herbst, R. W. Lee, and F. E. Pinkerton, Ann. Rev. Mater. Sci. 16,467 (1986).
[2] R. W. Lee, Appl. Phys. Lett. 46 ,790 (1985).
[3] K. S. V. L. Narashimhan, J. Appl. Phys. 57,4081 (1985).
[4] J. Inoue and M. Shimizu, J. Phys. F 16 ,1051 (1986).
[5] T. Itoh, K. Hikosaka, H. Takahashi, T. Ukai, and N. Mori, J. Appl. Phys. 61,3430 (1987).
[6] B. Szpunar, W. E. Wallace, and J. Szpunar, Phys. Rev. B 36 ,3782 (1987) .
[7] Z. Q. Gu and W. Y. Ching, Phys. Rev. B 36 ,8530 (1987).
[8] X. F. Zhong and W. Y. Ching, J. Appl. Phys. 67 ,4768 (1990).
[9] D. J. Sellmyer, M. A. Engelhardt, S. S. Jaswal, and A. J. Arko, Phys. Rev. Lett. 60 , 2077 (1988).
[10] S. S. Jaswal, Phys. Rev. B 41,9697 (1990).
[11] W. Kohn, and L. J. Sham, Phys. Rev. A1133 ,140 (1965)
[12] J. F. Herbst, J. J. Croat, F. E. Pinkerton, and W. B. Yelon, Phys. Rev. B29,4176 (1984).
[13] J. F. Herbst, J. J. Croat, and W. B. Yelon, J. Appl. Phys. 57 ,4086 (1985).
[14] J. P. Perdew, Y. Wang, Phys. Rev. B45 ,13244 (1992).
[15] J. P. Perdew, K. Burke, M. Ernzerhof, Phys. Rev. Lett. 77 ,3865 (1996) .
[16] P. Blaha, K. Schwar2, G. K. H. Madsen, K. Kvasnicka, J. Luitz, Wien2k, Karlheinz Schwarz, Technische Universitat wien, Austria “an Augmented Plane Wave + Local orbitals program for calculating crystal properties”, (2001).
[17] M.R.Norman, D.D.Koelling, and A.J.Freeman, Phys.Rev.B31, 6251 (1985)
[18] S.S.Jaswal, D.J.Sellmyer, M.Engelhardt, Z.Zhao, and A.J.Arko, Phys.Rev.B35, 996 (1987)
[19] J.F.Herbst and J.W.Wilkins, in Handbook on Physics and Chemistry of Rare Earths, edited by K.A.Gschneider, L.Eyring, and S.Hufner (Elsvier, New York, 1987), Vol.10, p.321.
[20] D. Givord anf H. S. Li, J. Appl. Phys. 57 ,4100 (1985).
[21] J. F. Herbst, J. J. Croat, and W. B. Yelon, J. Appl. Phys. 57,4086 (1985).
[22] D. Givord, H. S. Li, J.Appl.Phys.57,4100 (1985).